

Liquid Precursor-Based Synthesis of a weakly ordered carbon nitride with the composition C₂N

Nina Fechler ^{a*}, Niels P. Zussblatt ^b, Regina Rothe ^a, Robert Schlögl ^c, Marc-Georg Willinger ^c, Bradley F. Chmelka ^b, and Markus Antonietti, ^a

^a *Max Planck Institute of Colloids and Interfaces, Department of Colloid Chemistry, Research Campus Golm, 14424 Potsdam, Germany*

^b *University of California at Santa Barbara, Department of Chemical Engineering, Santa Barbara, California 93106, United States*

^c *Fritz Haber Institute of the Max Planck Society, Department of Inorganic Chemistry, Faradayweg 4-6, 14195 Berlin, Germany*

Abstract

Complexation of quinones and phenols with urea is shown to exhibit deep eutectic behavior which leads to liquid monomer mixtures at about 70 °C. These eutectic precursor mixtures are then converted to carbonaceous materials with well-defined structures and distributions of nitrogen heteroatoms. Due to the excellent wetting properties of the precursor mixtures, both hard- and salt-templating are possible, allowing the synthesis of highly porous carbonaceous materials with high surface areas along with simultaneous control over dopant functionality and pore architecture. When choosing a quinone educt containing no C-H bonds, condensation at comparably low temperatures leads to a novel type of nitrogen-containing carbon frameworks with a composition very close to C₂N and electronic conductivities of > 2 S/cm (following condensation at 800 °C). The structure of the material is analyzed by elemental analysis, porosimetry, HRTEM, EELS, and XPS where a disordered polymeric C₂N species composed of aromatic carbons and mainly pyrazinic nitrogens is in agreement with all data.

Introduction

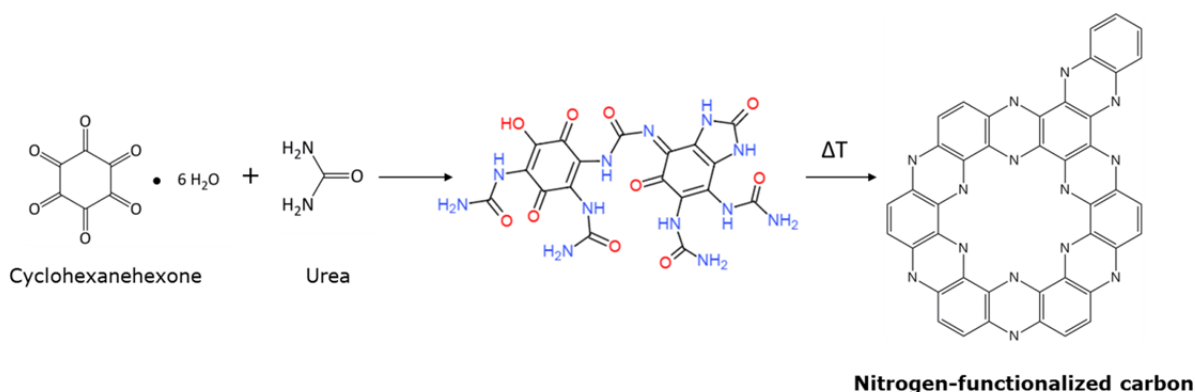
Nanocarbons, such as fullerenes, nanotubes, and graphenes, are versatile and promising materials whose properties depend essentially on their structure and surface composition.⁽¹⁾ Concerning porous carbons and electrode carbons, standard sustainable precursors include phenol-formaldehyde resins,⁽²⁻⁵⁾ carbohydrates, or even crude biomass, partly with selected composition.^(6,7) From a synthesis perspective, a significant processing advantage could be realized by applying recipes based on liquid precursors with little or no volatility, including ionic liquids ⁽⁸⁻¹⁰⁾ or deep eutectic mixtures.⁽¹¹⁾ Due to the liquid state, shaping and/or coating processes are more convenient, as is the use of templates to introduce defined porosity, then based on the polarity and miscibility with the liquid precursors. As a side effect, use of liquid precursors allow the convenient synthesis of nitrogen-,⁽¹²⁾ phosphorous-,⁽¹³⁾

boron-, (14) and/or sulfur-doped carbons (15), which have shown desirable properties including high oxidation stability (“noble carbons”), high conductivity, and varying degrees of (electro)catalytic activity.(16, 17) The reason for these improved electronic properties is still highly disputed,(18, 19) but control of local electron density and heteroatom distribution within the constituting graphene layers appears to be of key importance.(20, 21) However, fine structural control of the materials on the level of atomistic element patterns and their regularity has been difficult to achieve due to the inherent nature of liquid, randomly arranged molecules.

To expand on these techniques and combine the processability and homogeneity of liquids with the well-defined structure of prealigned liquid crystals, a new synthesis approach is presented based on supramolecularly pre-organized precursor mixtures composed of phenols/ketones, and urea. Due to strong hydrogen-bonding, these monomers form deep eutectic, partly liquid mixtures. Additionally, phenols and ketones are easily available, structurally flexible, and low-cost platform chemicals which are also a significant product of proposed biorefinery schemes (22-25). The second component, urea, one of the most used chemicals of the world, simultaneously serves as an effective nitrogen source and melting point depressing agent. In addition, it is possible to choose component precursor materials in a “mosaic-like,” co-condensation fashion which brings pre-organization, functionality, and heteroatom-doping to the target carbon material in a comparably simple and modular fashion.

The central aspect however lies in gaining improved chemical control over the entirety of the condensation process. This starts with the prerequisite of liquidity/plasticity in the first reaction stages, continues with adjustable wettability and the coupled possibility of coating and templating, and proceeds to the pre-orientation of the to-be-formed graphitic materials via supramolecular/liquid crystalline pre-condensates. Thus, this work seeks to bring the pyrolysis process (also referred to as “carbonization” or “coalification”), with its rather poor reputation concerning control and reproducibility, closer to concepts such as polycondensation (known from organic polymers), with improved reaction control. In other words, polymerization of nanocarbon materials including control of both atomistic chemical bonding patterns as well as nano- and micro structure is approached.

Within this much broader concept beside model compounds, we exemplarily focus in this paper on the condensation of urea with cyclohexanhexone, a precursor without any C-H-bond. The different reaction steps and the resulting materials are characterized by X-ray diffraction (XRD), nuclear magnetic resonance spectroscopy (NMR), elemental analysis, high resolution electron microscopy, Electron Energy Loss Spectroscopy (EELS), and X-ray photoelectron spectroscopy (XPS). Combined understanding from these techniques indicates a covalent, fully aromatic carbon/nitrogen-material (“carbon nitride”) with the approximate composition of C₂N, high homogeneity, and the nitrogen predominantly present as pyrazine units. An idealized scheme of this reaction is presented in Scheme 1:



Scheme 1: Condensation scheme of cyclohexanehexone with urea to highly nitrogen-functionalized carbons.

Materials and Methods

Synthesis:

The chemicals 1,2-dihydroxybenzene (Sigma Aldrich, 105 °C decomposition), 2,5-dihydroxy-1,4-benzoquinone (Alfa Aesar, 220 °C sublimation), cyclohexanehexone (Sigma Aldrich, 99 °C decomposition) and urea (133 °C melting point) were used as received. To prepare 1,2-benzoquinone from 1,2-dihydroxybenzene, 0.5 g of 1 M NaOH solution was added to 5 g of 1,2-dihydroxybenzene under stirring and kept overnight to form dark blue crystals. In a typical synthesis of a nitrogen-doped supramolecular carbonaceous material, stoichiometric amounts of the phenol/quinone and urea are mixed such that all oxo- groups are saturated by urea, i.e. cyclohexanehexone : urea 1:3, 1,2-benzoquinone : urea 1:1, 2,5-dihydroxy-1,4-benzoquinone : urea 1:2. Deep eutectics were formed through gentle heating of the powder mixtures in a glass vial to temperatures between 90 °C and 135 °C (2,5-dihydroxy-1,4-benzoquinone:urea 1:2), respectively. For the synthesis of the carbons, the eutectic mixtures were heated to varying temperatures under nitrogen flow with a heating rate of 2.5 °C min⁻¹ and kept for 1 h at the final temperature.

Porous versions of the carbons were prepared from the precursor mixture of cyclohexanehexone and urea in a 1:3 mole ratio using SBA-15 or ZnCl₂ as templates. For SBA-15: After heating the precursor mixture (1366 mg) at 90 °C to form a liquid, 1 ml of water for reduced viscosity and 350 mg of SBA-15 were added and infiltrated under reduced pressure. For the salts: after heating the precursor mixture at 90 °C to form a liquid followed by cooling in an open vial, the re-solidified precursor was mixed with ZnCl₂ in a weight ratio of precursor : salt of 1:0.5 to 1:16, respectively. After heat treatment, the crude products were grinded and SBA-15 removed through stirring overnight in 250 mL of 1 M NaOH solution whereas salts were removed through washing in 1 L of water followed by washing in 1 M HCl. All products were finally dried in a vacuum oven at 50 °C.

The materials described herein are named as SCM-x-y, where SCM stands for supramolecular carbonaceous materials; x denotes the number of phenol/oxo-groups of the starting quinone educt, and y the synthesis condensation temperature.

Characterization:

Bulk elemental composition was determined using combustion analysis using a Vario Micro device. Wide angle X-ray-patterns were taken on a Bruker D8 Advance instrument using Cu-K α -radiation. Differential scanning calorimetry (DSC) was performed with a Mettler Toledo DSC 1 STARe System under nitrogen atmosphere. The samples were run in an aluminum crucible in a sealed furnace and heated to 200 °C with heating rate of 5 °C min⁻¹. Subsequently, the samples were cooled down at the same rate. TEM images were obtained on a Zeiss EM 912 Ω instrument and SEM images on a LEO 1550-Gemini instrument after sputtering with platinum. High resolution TEM images and EELS spectra were recorded using a double Cs corrected JEOL ARM 200F instrument. Since the material demonstrated a very high stability against electron beam damage, the microscope was operated at 200kV.

Nitrogen sorption measurements were performed using N₂ at 77 K after degassing the samples at 150 °C under vacuum for 20 hours with a Quantachrome Quadrasorb SI porosimeter. The surface area was calculated by applying the Brunauer-Emmett-Teller (BET) model to the isotherm data points of the adsorption branch in the relative pressure range $p/p_0 < 0.3$ in the linear region with the best correlation. The pore size distribution was calculated from N₂ sorption data using the nonlocal density functional theory (NLDFT) equilibrium model method for slit pores provided by Quantachrome data reduction software QuadraWin Version 5.05.

TGA-MS

AFM

Liquid state ¹H NMR spectroscopy was carried out at room temperature on a Bruker DPX-400 spectrometer operating at 400.1 MHz with spectra consisting of the average of 10000 scans collected with an acquisition time of 3.0 s. For the measurement 20 mg of sample were dissolved in 0.7 ml of deuterated dimethyl sulfoxide (DMSO). The solvent peak was used for calibration.

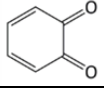
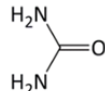
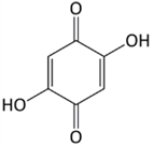
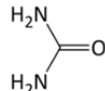
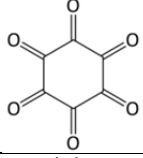
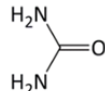
Surface compositions of the materials were characterized by X-ray photoelectron spectroscopy (XPS) using a Kratos Axis Ultra X-ray photoelectron spectroscopy system. These measurements characterized the elemental composition of the exterior 8-10 nm of sample particles with 0.1 atom% resolution. Surface elemental compositions were determined using survey scans over a range of 1200 to 0 eV with a step size of 0.5 eV and a pass energy of 160 eV. Quantitative characterization of the presence of various nitrogenous sites was accomplished using high-resolution nitrogen XPS, scanning over a range of 413 to 390 eV with a step size of 0.05 eV and pass energy of 20 eV. Spectra were processed using CasaXPS software, and each distribution recorded by the high-resolution N scan was deconvoluted into multiple

Gaussian lineshapes based on the binding energies of electrons associated with nitrogens in various functional groups.(26)

Results and discussion

First, the ability to form eutectic mixtures of the three phenols/ketones with urea was explored, however restricted to stoichiometric compositions allowing further condensation, i.e. two hydroxyl- and/or oxo-groups, were adjusted per two nitrogen moieties of the urea. By the choice of the monomer cyclohexanehexone and two model compounds (Table 1), it was attempted to cover a rather wide range of aggregation structures, including locally interacting, "0D"- stacked discotic entities produced with 1,2-benzoquinone (SCM-2-y), "1D", linear aggregated, polymeric materials synthesized with 2,5-dihydroxy-1,4-benzoquinone (SCM-4-y), and "2D"- extended aggregation networks from cyclohexanehexone (SCM-6-y). Note that the materials synthesized from cyclohexanehexone and urea (SCM-6-y) do not contain any C-H linkages, which will be shown to simplify the further thermal transformations as the aromatic C-H bond is very strong and thus usually counteracts condensation. Structures of precursors and some representative composition data for materials prepared at various condensation temperatures are presented in Table 1. Note that the sum of weight percent does not equal 100% which is likely due to the high stability and thus incomplete combustion of the samples. This is also supported by elemental analysis from XPS which reveals low oxygen contents for the condensed materials (Supporting Information: Table SI-1 XPS surface composition data).

Table 1: Precursor ratios, eutectic melting points and elemental composition following condensation of supramolecular carbonaceous materials at varying temperatures.

Label	Precursor components		Molar mix-ratio	Mix-melting point [°C]	Condensation temperature (y) [°C]	Elemental composition of SCM [wt%]				
	1	2				N	H	C	C/N	
SCM-2-y	 1,2-benzoquinone		1:1	68.5	90	13.0	5.6	49.1	3.1	
					500	31.0	2.5	49.0	1.6	
					800	12.5	1.3	76.0	6.1	
SCM-4-y	 2,5-dihydroxy-1,4-benzoquinone			1:2	129	135	22.3	4.3	39.3	1.7
						500	18.0	2.5	64.0	3.5
						800	15.0	1.9	75.0	5.0
SCM-6-y	 cyclohexanehexone			1:3	68.0	90	22.0	4.0	29.0	1.3
						500	36.0	2.0	52.0	1.4
						800	28.0	1.3	63.0	2.2

The diverse phenomena occurring during the synthesis process are representatively shown for the cyclohexanehexone and urea based materials (SCM-6-y) in Figure 1 a-c. Starting from a powder mixture of cyclohexanehexone and urea (Figure 1 a), liquefaction occurs below the melting point of the respective components (here 68 °C), indicating the formation of a deep eutectic medium, simultaneously with a color change from beige to dark orange upon gentle warming (Figure 1 b insert). The mixture can be easily undercooled and shows in polarization microscopy birefringence typical for liquid crystalline mixtures (Figure 2 b). This already indicates the development of a highly stacked, aromatic charge-transfer system even without any carbonization, i.e. the electronic coupling of the monomer units towards larger, preorganized assemblies. During this process, the evolution of water and gases from monomer condensation and potential decomposition is observed. Reactivity increases with increasing amounts of hydroxyl- and/or oxo-groups.

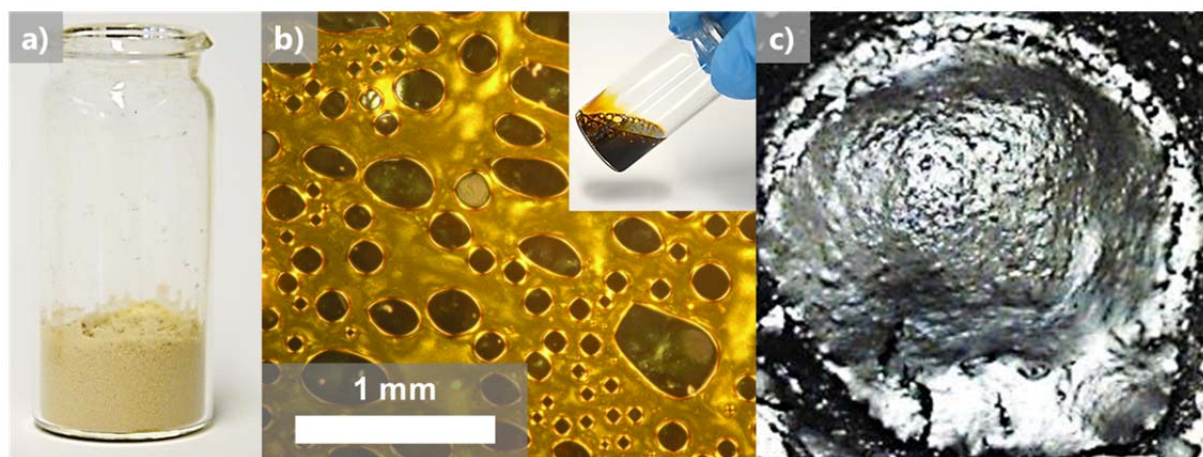


Figure 1: Photographs of the synthesis process: (a) powder of the cyclohexanehexone:urea mixture at room temperature, (b) Optical microscope of the liquid crystalline eutectic mixture in the undercooled liquidus, partial polarization mode (insert: macroscopic view), (c) cohesive, silvery reflecting monolithic carbon foam after condensation at 500 °C.

For 1,2-benzoquinone and urea (SCM-2-90) cooling generates an ordered crystalline solid (Figure SI-1 d, e) while in the case of 2,5-dihydroxy-1,4-benzoquinone and urea condensation occurs along with related viscosity increase similar to cyclohexanehexone-based materials, first forming sticky plastic states which can be pressed to films or spun to fibers (Figure SI-2). Finally, the systems adopt a resin-like state which suggests the development of an extended network structure, presumably both via covalent linkages and very strong hydrogen-bridges. Adjustment of viscosity by addition of water was determined to be a processing option in most cases, though local order and organization might be influenced.

Further condensation at 500 °C leads to carbons of varying appearance which again can be related to the diverse modes of preorganization. While the material prepared from 1,2-benzoquinone (SCM-2-500) forms black needles, those synthesized from precursors with greater numbers of hydroxyl- or oxo- groups (see SCM-6-500, Figure 1 c) are silvery-black carbons with pronounced metallic gloss and a cohesive, “cupcake-like” morphology which is stronger for the six-valent species. It is to be

noted that the formation of such metallic or graphite-like states already at 500 °C is very unusual and is regarded as a key advantage of the described synthesis.

It is important to note that the as-determined elemental compositions of the materials synthesized by condensation at 500 °C are very close to reaction products formally obtained by the removal of all condensable water molecules, i.e. a "C_{0.6}N_{0.4}" for the SCM-6-500 species and a "C_{0.66}N_{0.33}" for the SCM-4-500 species, indicating that urea and the quinones readily condense in a first step via water elimination towards the black-silver polymer resin-like species. It should be also stated that by composition (even assuming complete water elimination) the 500 °C structures are "oxygen-poor", i.e. there is a second oxygen elimination reaction active already at comparably low temperatures.

TGA-MS measurements were performed to support this molecular picture and significantly only the elimination products H₂O followed by CO and N₂ could be identified (Figure SI-3). At temperatures higher than 700 °C this is followed by combustion processes due to residual oxygen. This product pattern is in agreement with a proposed condensation mechanism eliminating first water, then the excess of urea fragments.

XRD patterns (Figure 2) are in good agreement with the visual appearance. The 1,2-benzoquinone- and urea-based material (SCM-2-90) exhibits well-defined diffraction patterns, confirming the presence of larger precursor crystals. Those crystals are not the focus of the present manuscript, but serve as a low molecular weight model to provide some insights into the reaction mechanism. Materials synthesized with precursors having more hydroxyl- or oxo-groups (SCM-4-135 Figure SI-4, and SCM-6-90 Figure 2) exhibit broad peaks typical for liquids or polymers. SCM-6-90 reveals a second broad peak around 14° which has been attributed to the in-plane ordering of the H-bridged complexes. This is supported by the ¹H liquid NMR of SCM-6-90 where very high signals between 10.5 – 12.0 ppm hint to strong dipole-coupling between stacked and highly organized polarizable layers (Figure SI-5) even in the liquid state. These aggregates can be also nicely observed by AFM (data not shown here) where the whole sample reveals a composition of thin primary flake-like aggregates with about 1 nm in thickness. The XRD- reflection centered approximately 26° is usually attributed to the stacking of aromatic systems,(27) also supported by the black and orange charge-transfer colors of SCM-4-135 and SCM-6-90, respectively.

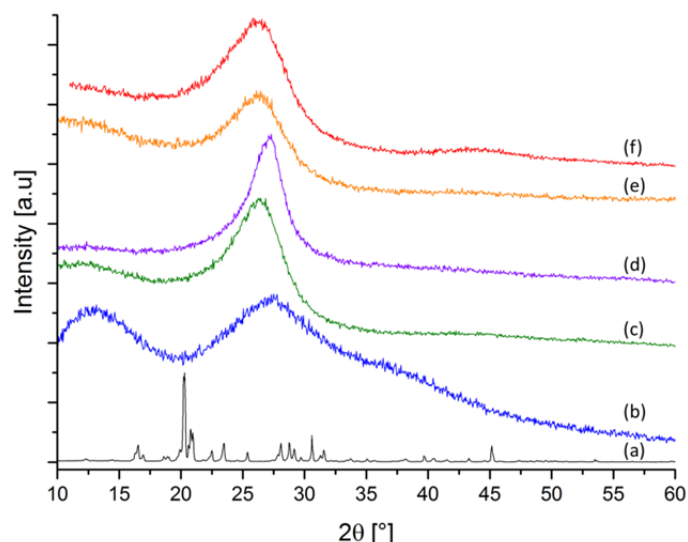


Figure 2: X-ray diffraction patterns of supramolecular carbonaceous materials based on 1,2-benzoquinone/urea and cyclohexanehexone/urea at varying condensation temperatures: (a) SCM-2-90 (black), (b) SCM-6-90 (blue), (c) SCM-6-500 (green), (d) SCM-6-500-ZnCl₂ (violet), (e) SCM-6-700 (orange) and (f) SCM-6-800 (red).

Treatment at elevated temperatures leads to X-ray diffractograms with more pronounced aromatic stacking peaks, typical of graphitic carbons, concurrent with development of the in-plane signal at around 43°. This reflects the progressing condensation and thus extension of the aromatic system. The fast cross-linking at early reaction-stages and therefore high stability is also supported by unusually high reaction yields (70-98 wt% and 10-30 wt% at low and high synthesis temperatures, respectively) as well as unusually high preservation of nitrogen content (Table 1). The outstanding value of 30 wt% nitrogen for the cyclohexanehexone and urea based material condensed at 800 °C (SCM-6-800) indicates that the initial nitrogen patterning can be preserved even at elevated temperatures. Note that the ideal “C₂N” depicted in Scheme 1 would be characterized by 33 mol% of nitrogen that is indeed very close to its polymeric version. Retention of heteroatoms in specific positions is highly desired since they are expected to introduce electronic defects which can improve electrocatalytic properties, and they have been found to improve performance when such materials are employed e.g. as supercapacitor electrodes.⁽²⁸⁾ This is also reflected by comparison of the diffractograms of cyclohexanehexone-based materials at different temperatures (SCM-6-y) in which only gradual changes in order and peak position are observed (Figure 3 d-f), indicating that the local structure is essentially just slightly reshuffled throughout the condensation process.

Here, it is noted that the solid state NMR-investigation of nitrogen-containing carbons is not trivial because of high electronic conductivity, and had failed in many cases. A more detailed investigation of the materials with this technique was performed and agrees with our structural models, however, data will be presented in all details in a following independent manuscript. To assist with the identification of nitrogenous functional groups present in these materials, high-resolution nitrogen XPS was performed on the natural abundance analogue materials. Deconvolution of the N 1s peak according to electron binding energies suggests that the 500 and

800 °C condensed materials are both primarily composed of pyridinic/pyranizinic and pyrrolic nitrogen species, as shown in Table 2. Graphitic (also referred to as "quaternary") nitrogen and nitroxide species which exhibit greater stability at higher condensation temperatures are minorities in both materials, though their proportions increase at higher condensation temperatures. This is very exciting, as the only way to embed 20 mol% of nitrogen in pyrazinic sites without any C-H- bonds is in a structure very similar to the idealized one presented in Scheme 1. Structural imperfections and non-closed rings/surface termination is then accomplished via the 7mol% of pyrrolic sites. It is to be underlined that XPS is a surface sensitive technique, i.e. the 7 mol% pyrrolic sites include all necessarily existing surface terminations, however, the structural bulk order is presumably significantly higher.

Table 2: Characterization of surface nitrogenous species of cyclohexanehexone- and urea-based materials (SCM-6-y) synthesized with 500 and 800 °C condensation temperatures from high-resolution N XPS, including overall and relative percentage of nitrogen in the material.

<i>Condensation temperature [°C]</i>	<i>Absolute and relative surface nitrogen species compositions</i>	
	500	800
overall N	31.0 at% (100%)	22.5 at% (100%)
pyridinic N	20.7 at% (67%)	10.3 at% (46%)
pyrrolic N	7.0 at% (23%)	6.0 at% (27%)
graphitic N	2.4 at% (8 %)	4.1 at% (18%)
nitroxide	0.9 at% (3%)	2.2 at% (10%)

To demonstrate the versatility and processability of the SCM-approach not only on the level of the atomistic control of carbon structure and substitution patterns, the micro- and nanoarchitecture of the materials was synthetically controlled towards different useful morphologies. Representatively performed with the urea- and cyclohexanehexone-based system produced with high-temperature condensation (SCM-6-800), structures ranging from ordered mesopores with very high surface area to zeolite-like materials can be obtained by using either SBA-15 as a hard template or salt templating/salt melt synthesis, respectively.(29) Transmission electron microscopy images reveal that both templating methods can be successfully employed for the morphosynthesis of very differently structured but highly porous nitrogen-containing carbon materials. For the material produced with SBA-15 (SCM-6-800-SBA-15) even the typical negative line pattern structure of the initial template can be observed (Figure 3 a).

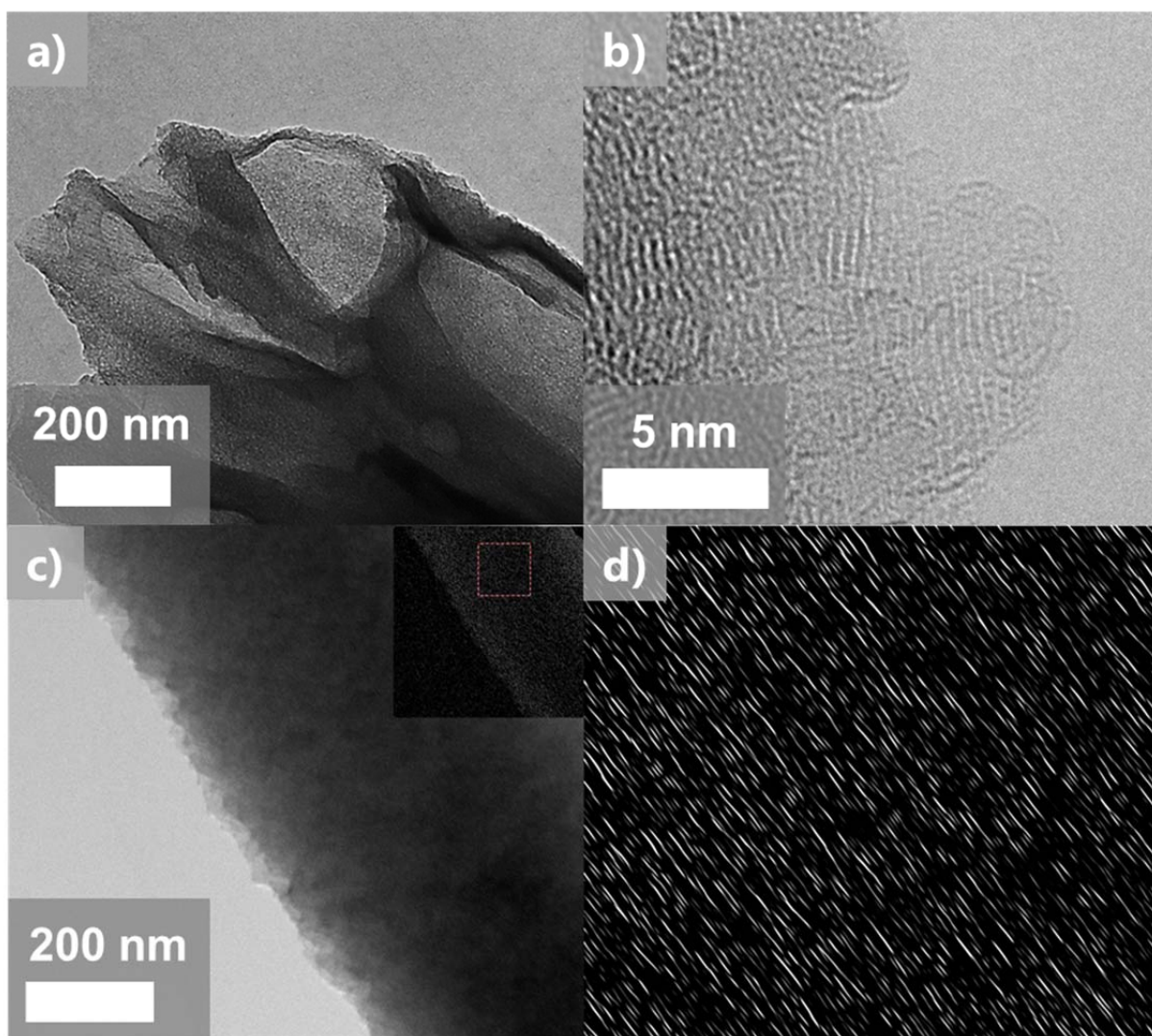


Figure 3: Transmission electron microscopy of morphosynthesis experiments with supramolecular carbonaceous materials based on cyclohexanehexone/urea to illustrate the structuring of the preorganized monomer mixtures: (a) templated with SBA-15, “ordered mesoporous” (b-d) templated with ZnCl_2 salt melt for well accessible micropores, b) high resolution image showing local structural order. c) overview image and d) Fourier-filtered image abstracted from the region shown in the inset of c), highlighting structural ordering.

The presence of sufficiently thin morphologies also enables the application of aberration corrected high resolution electron microscopy (HR-TEM) for the final characterization also of weakly ordered samples. Figures 3 b-d show that already at 700 °C samples made in ZnCl_2 salt melt are essentially composed of nicely stacked but partly bended graphitic layers with the typical stacking distance of 0.35 nm, as already found in the XRD experiments. The fact that also the thicker grains are composed of lamellar substructures is visible in the pictures, but can be further elaborated by electron diffraction and Fourier-filtered reconstituted pictures (Figure 3 c and d). Contrary to classical carbon nitride samples (i.e. C_3N_4) or ordinary amorphous carbons, the samples are highly stable under the electron beam.

Nitrogen sorption experiments essentially reveal in addition successful templating by the SBA-15 silica as well as the formation of high surface area or oligo-stacked “C₂N”-layers (Figure 4). It must be noted that the synthesis of an efficient porous system mostly relies on a template where the structure can be synthesized around. Salt templating has turned out to be remarkably successful in the context of well-defined carbon structures.(10)

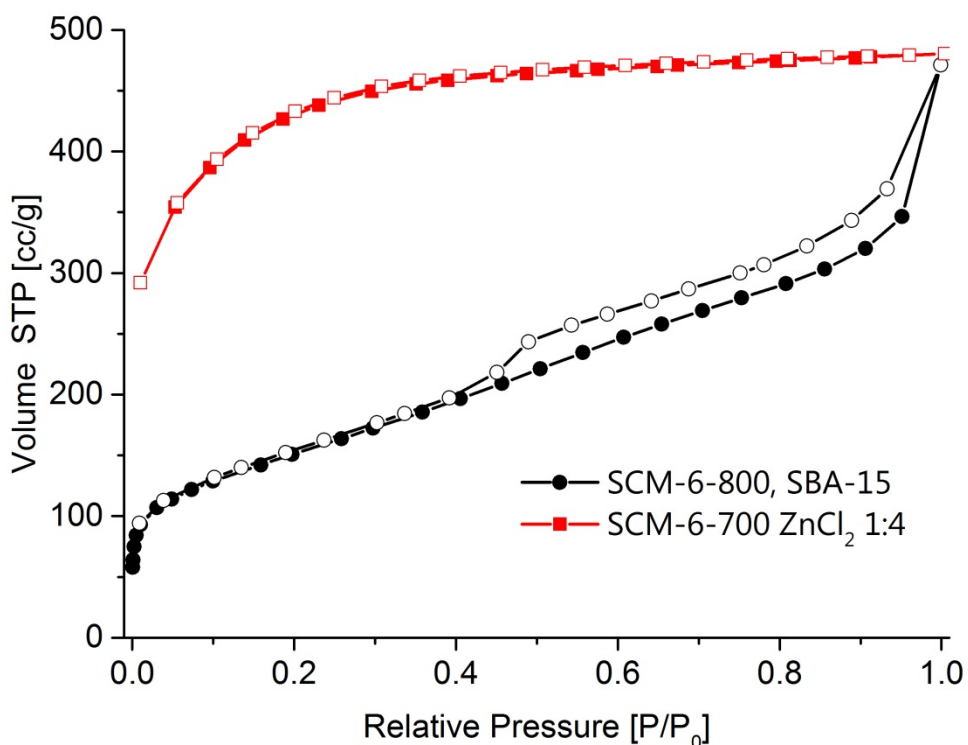


Figure 4: Nitrogen sorption isotherms of supramolecular carbonaceous materials based on cyclohexanehexone/urea templated with SBA-15 (black, circle) or ZnCl₂ (red, square). Solid indicates adsorption branch, hollow indicates desorption branch.

Especially in templated samples, beside the outer structural surface area also micropores are in addition well accessible contributing to the majority of surface area. This very nicely corroborates a structural model of porous layers where the pores are lined by pyrazinic nitrogens. This very high specific surface area (1512 m²g⁻¹ of this specific sample) together with the morphology observed in HR-TEM strongly hint to single layers which are densely packed with zeolite-like pores.

EELS finally reflects the hybridization state around the two composing elements, i.e. carbon and nitrogen (further elements including oxygen are not observed, Figure 5).

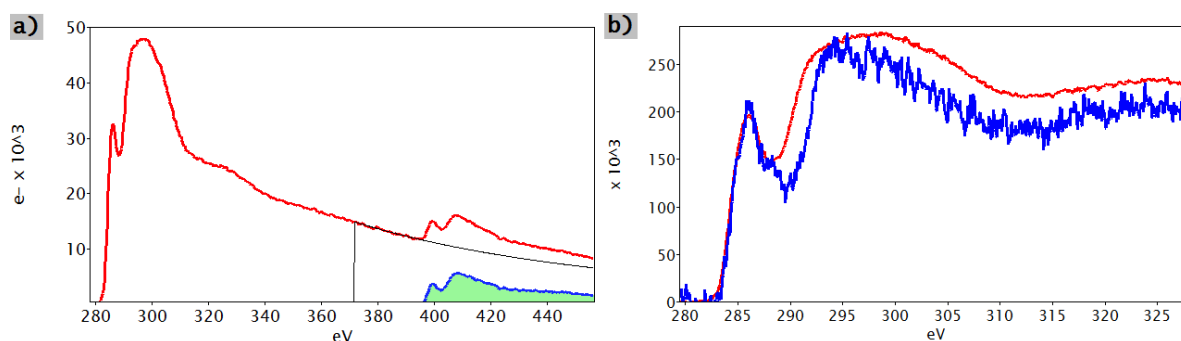


Figure 5: EELS of supramolecular carbonaceous materials based on cyclohexanehexone/urea templated with ZnCl_2 .

EELS spectra recorded from the supramolecular carbonaceous material over the energy range of the carbon K and nitrogen K-edges are shown in Figure 5a. Both, the carbon K- and nitrogen N-edges show clear π^* and σ^* features and from the integral intensity of the respective edges, an elemental C/N ratio of roughly 80/20 can be estimated (see SI). The fine structure of the carbon K edge reflects defective, sp^2 -hybridized carbon with amorphous contributions. Compared to the carbon K-edge, the nitrogen edge shows more developed features in the π^* region, reflecting different N types, a more pronounced valley between the π^* and σ^* -features as well as a less broadened σ^* feature, reflecting a higher degree of sp^2 -ordering. The EELS fine structure contains information about the electronic structure at and in the surrounding of the ionized species. Hence, it can be assumed that the nitrogen atoms share the electronic structure with a portion of the carbon that is more ordered than what is reflected in the carbon K-edge. Excessive carbon that is found to be present by the EELS quantification therefore contributes to the amorphous portion of the carbon K-edge, while the nitrogen K-edge indicates that the special precursor bonding motif is kept throughout the condensation process. The nitrogen edge is also mainly the one of sp^2 -coordinated nitrogen within the sp^2 -carbon pool. Additionally, a slight overlay with a second electronic structure is present, which is, however, potentially due to the already discussed surface terminations. Overall, also the EELS data nicely support the suggested structure model of a slightly defective C_2N structure, as initially depicted in Scheme 1.

To illustrate the semi-metallic character of the uniform carbon/nitrogen arrays generated by the present approach already at comparably low synthesis temperatures, conductivity measurements were performed for SCM-6-800. A value of 2 S cm^{-1} at 423 K was obtained for a sintered pellet, while Seebeck measurements clearly indicate the dominant n-character of the charge transport. The details of these electronic measurements would however exceed the limits of this publication and are subject to forthcoming work.

Conclusion

This article presents the synthesis of a new carbon-nitrogen materials starting from a deep eutectic mixture of cyclohexanehexone as a structure donating motif and urea as a melting point depressant as well as nitrogen-source. As followed by elemental analysis, XRD, HR-TEM, EELS, and XPS condensation of these two reactants occurs in a structurally rather organized fashion. Eventually this results in carbonaceous condensates with metallic gloss starting from reaction temperatures as low as 500 °C. The product condensed at 700 – 800 °C can be rather nicely described as a disordered version of “C₂N” with a nitrogen content of 31 mol% and a predominance of pyrazinic positions where pyrrolic nitrogens are present for surface termination and as defect structures. At the end, Markus will appraise the added HRTEM and sorption facts..

Acknowledgements

The work at UCSB was supported by the USARO through the Institute for Collaborative Biotechnologies under contract no. W911NF-09-D-0001. The authors thank Gylhaine Clavel for HRTEM measurements, Laurent Chabanne for TGA-MS measurements and Hubert Gojzewski and Rodrigo Pérez-García for AFM measurements. This work was partially supported by the IMI Program of the National Science Foundation under Award No. DMR 0843934, and the UCSB-MPG Program for International Exchange in Materials Science.

References

- [1] H.-P. Cong; J.-F. Chena; S.-H. Yu, *Chem. Soc. Rev.*, 2014, DOI: 10.1039/C4CS00181H
- [2] J. Liu, T. Yang, D.-W. Wang, G. Q. (M.) Lu, D. Zhao, S. Z. Qiao, *Nat. Commun.* 2013, 4, 2798.
- [3] J. Liu, S. Z. Qiao, H. Liu, J. Chen, A. Orpe, D. Zhao, G. Q. (M.) Lu, *Angew. Chem. Int. Ed.*, 2011, 50 5947.
- [4] Wei Li , Qin Yue , Yonghui Deng , * and Dongyuan Zhao, *Adv. Mater.* 2013, 25, 5129.
- [5] A. Vu, X. Li, J. Phillips, A. Han, W. H. Smyrl, P. Bühlmann, A. Stein, *Chem. Mater.* 2013, 25, 4137.
- [6] L. Zhao, L.-Z. Fan, M.-Q. Zhou, H. Guan, S. Qiao, Markus Antonietti, M.-M. Titirici, *Adv. Mater.*, 2010, 22, 5202.
- [7] R. J. White, N. Brun, V. L. Budarin, J. H. Clark, M.-M. Titirici, *Chem. Sus. Chem.* 2014, 7, 670.
- [8] J. P. Paraknowitsch, A. Thomas, *Macromol. Chem. Phys.*, 2012, 213, 1132.

- [9] J. Seung Lee, X. Wang, H. Luo, S. Dai, *Adv. Mater.* 2010, 22, 1004.
- [10] N. Fechler, T.-P. Fellingner, M. Antonietti, *Adv. Mater.* 2013, 25, 75.
- [11] D. Carriazo, M. C. Serrano, M. C. Gutierrez, M. L. Ferrer F. del Monte, *Chem. Soc. Rev.*, 2012, 41, 4996.
- [12] S. Dai et al, *Chem. Sus. Chem.*, 2012, 5, 1912.
- [13] J. P. Paraknowitsch, Yuanjian Zhang, Björn Wienerta, A. Thomas, *Chem. Commun.*, 2013, 49, 1208.
- [14] P. F. Fulvio, J. S. Lee, R. T. Mayes, X. Wang, S. M. Mahurina S. Dai, *Phys. Chem. Chem. Phys.*, 2011, 13, 13486.
- [15] N. Fechler, T.-P. Fellingner, M. Antonietti, *J. Mater. Chem. A*, 2013, 1, 14097.
- [16] T.-P. Fellingner, D. S. Su, M. Engenhorst, De. Gautam, R. Schlögl, M. Antonietti, *J. Mater. Chem.*, 2012, 22, 23996.
- [17] W. Yang, T.-P. Fellingner, M. Antonietti, *J. Am. Chem. Soc.* 2011, 133, 206.
- [18] J. Liang, Y. Jiao, M. Jaroniec, S. Z. Qiao, *Angew. Chem.* 2012, 124, 1.
- [19] Y. Jiao, Y. Zheng, M. Jaroniec, S. Z. Qiao, *J. Am. Chem. Soc.* 2014, 136, 4394.
- [20] L.-F. Chen, Z.-H. Huang, H.-W. Liang, H.-L. Gao, S.-H. Yu, *Adv. Funct. Mater.* 2014, 24, DOI 10.1002/adfm.201400590.
- [21] D. S. Dhawale, G. P. Mane, S. Joseph, C. Anand, K. Ariga, A. Vinu, *Chem. Phys. Chem*, 2013, 14, 1563.
- [22] J. Zakzeski, P. C. A. Bruijninx, A. L. Jongerius, B. M. Weckhuysen, *Chem. Rev.* 2010, 110, 3552.
- [23] V. Molinari, C. Giordano, M. Antonietti, D. Esposito, *J. Am. Chem. Soc.* 2014, 136, 1758.
- [24] Paola Ferrini and Roberto Rinaldi, *Angew. Chem. Int. Ed.* 2014, 53, 1.
- [25] B. Joffres C. Lorentza, M. Vidalieb, D. Laurentia*, A.-A. Quoineaadb, N. Charonb, A. Daudinb, A. Quignardb, C. Geantet, *Appl. Catal. s B: Environmental*, 2014, 145, 167.
- [26] Jansen, R. J. J.; van Bekkum, H., *Carbon* 1995, 33, 1021; Dorjgotov, A.; Ok, J.; Jeon, Y.; Yoon, S. H.; Shul, Y. G., *J. Appl. Electrochem.* 2013, 43, 387
- [27] K. P. Gierszal, M. Jaroniec, T.-W. Kim, J. Kim, R. Ryoo, *New J. Chem.* 2008, 32, 981
- [28] K. Jurewicz, K. Babeł, A. Żiółkowski, H. Wachowska, *Electrochim. Acta* 2003, 48, 1491

[28] X. F. Liu, N. Fechner, M. Antonietti, Salt melt synthesis of ceramics, semiconductors and carbon nanostructures. *Chem. Soc. Rev.* 42 (21), 8237-8265 (2013)

Supporting Information

A Liquid Precursor Platform Based on Defined Quinones to Synthesize Carbon Materials with unique Heteroelement Patterns

Nina Fechler ^{a*}, Niels P. Zussblatt ^b, Regina Rothe ^a, Markus Antonietti, ^a and Bradley F. Chmelka ^b

^a Max Planck Institute of Colloids and Interfaces, Department of Colloid Chemistry, Research Campus Golm, 14424 Potsdam, Germany

^b University of California at Santa Barbara, Department of Chemical Engineering, Santa Barbara, California 93106, United States

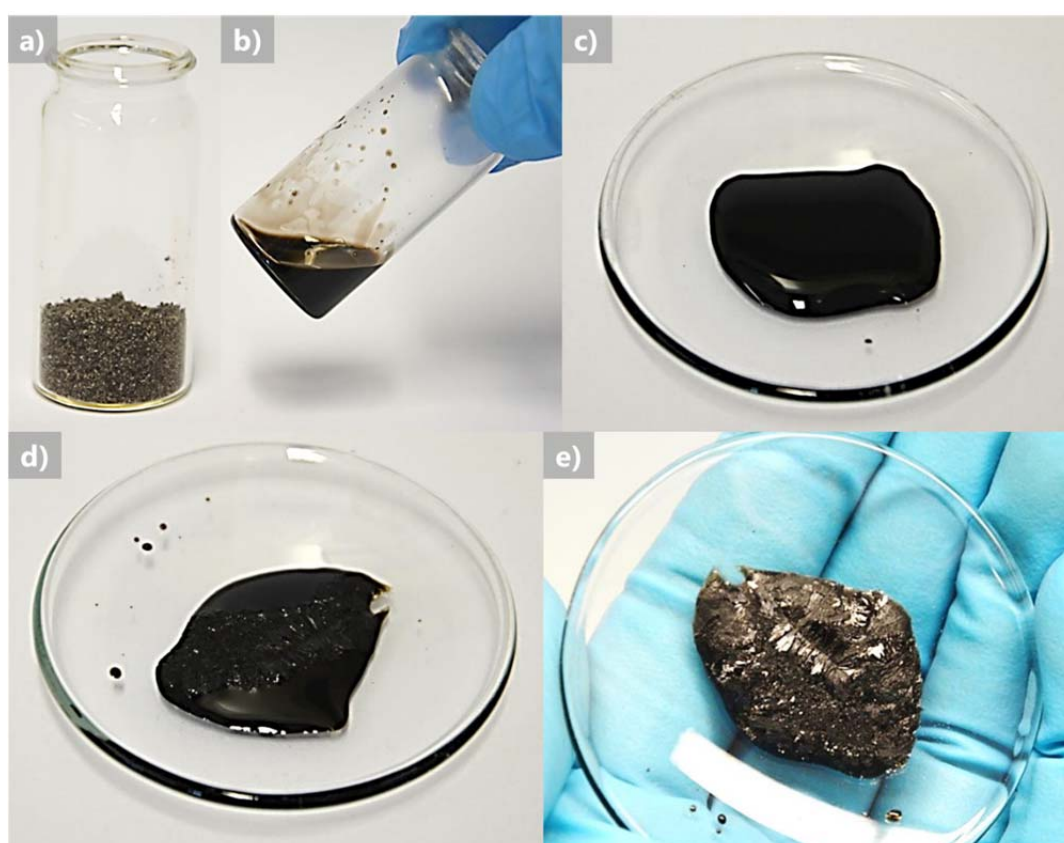


Figure SI-1: Photographs of the synthesis process of the 1,2-benzoquinone and urea based system (SCM-2-y): (a) powder of the 1,2-benzoquinone:urea mixture at room temperature, (b, c) powder-to-liquid transition at 90 °C (SCM-2-90), (d) onset of crystallization upon cooling back to room temperature finally resulting in a crystalline solid (e).

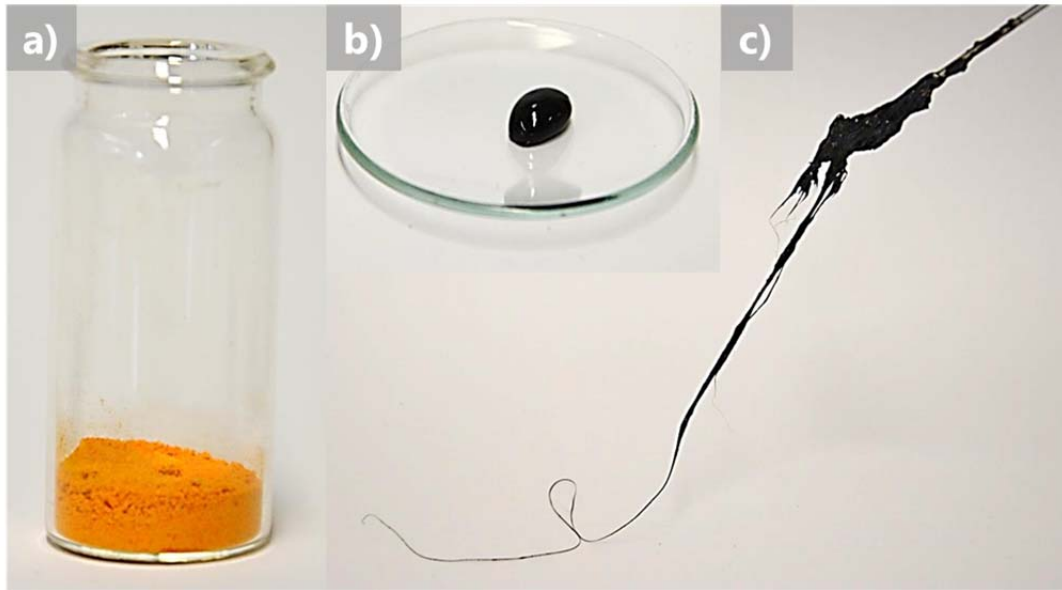


Figure SI-2: Photographs of the synthesis process of the 2,5-dihydroxy-1,4-benzoquinone and urea based system (SCM-4-y): (a) powder of the 2,5-dihydroxy-1,4-benzoquinone:urea mixture at room temperature, (b) powder-to-liquid transition at 135 °C (SCM-4-135), (c) plastic, processable intermediate.

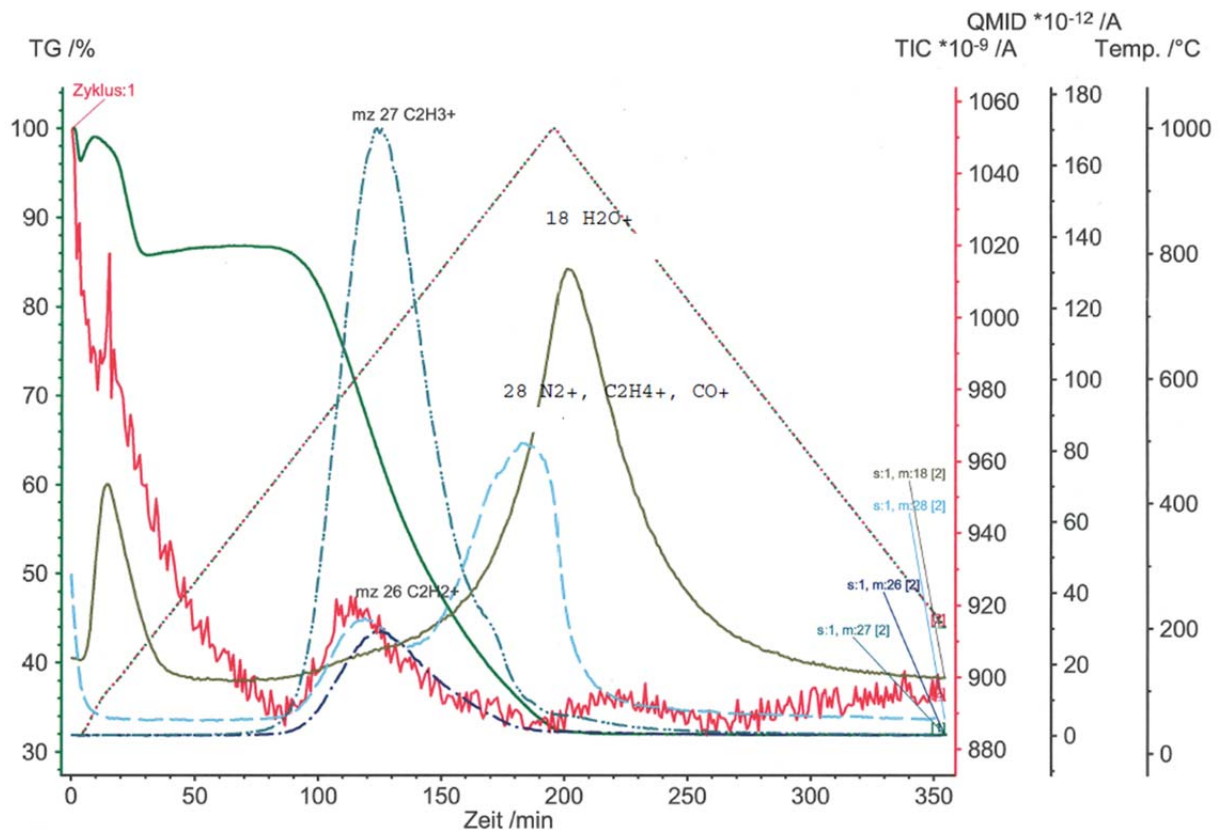


Figure SI-3: TGA-MS measurement of cyclohexanehexone and urea powder mixture.

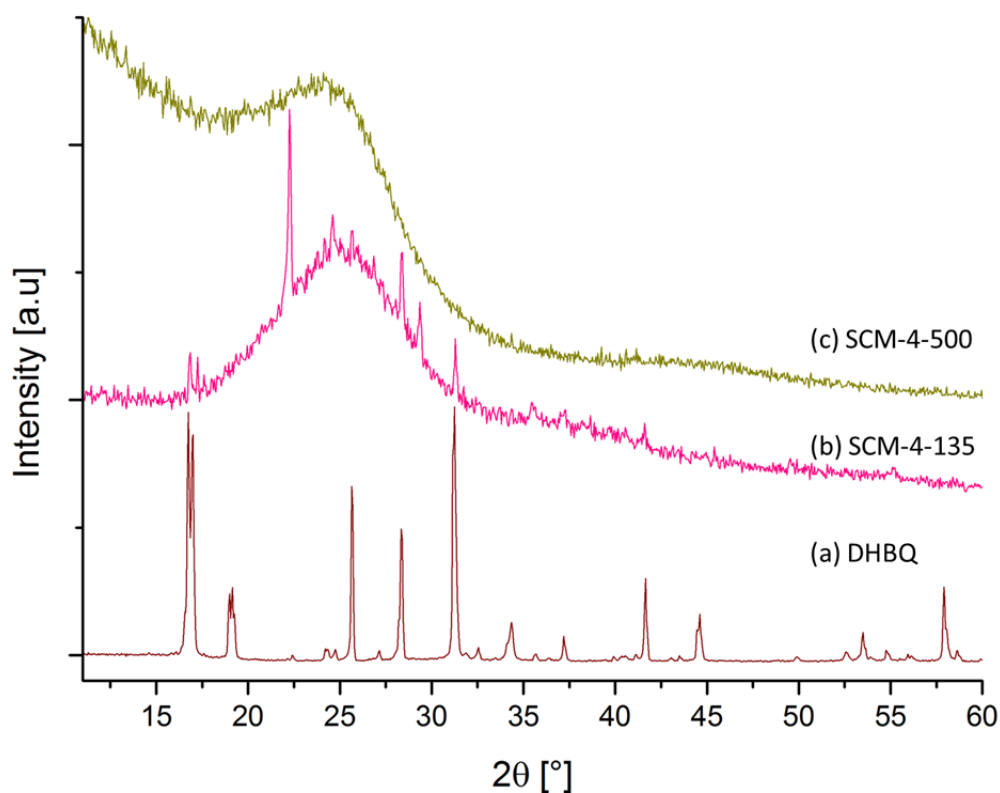


Figure SI-4. X-ray diffraction patterns of (a) 2,5-dihydroxy-1,4-benzoquinone (DHBQ, wine-red) and supramolecular carbonaceous materials based on 2,5-dihydroxy-1,4-benzoquinone at varying condensation temperatures (b) SCM-4-135 (pink), (c) SCM-4-500 (olive).

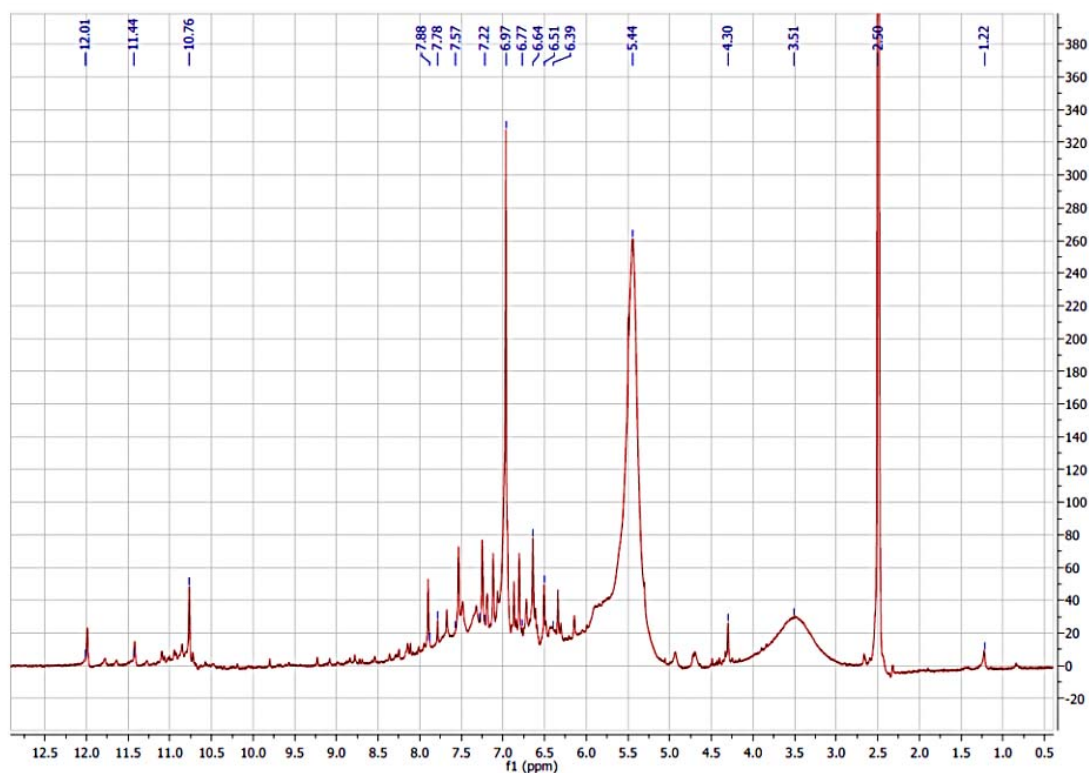


Figure SI-5. $^1\text{H-NMR}$ of cyclohexanehexone- and urea-derived material after 90 °C (SCM-6-90) in DMSO.

Table SI-1. X-ray photoelectron spectroscopy (XPS) surface elemental composition of cyclohexanehexone- and urea-derived materials (SCM-6-y) at various pyrolysis temperatures (y).

<i>Condensation temperature (y) [°C]</i>	<i>Surface elemental composition [atom%]</i>		
	C	N	O
90	46.9	19.0	34.1
500	63.7	31.0	5.3
800	73.3	22.5	4.1